Radiolabeled oligosaccharides nanoprobes for infection imaging

Jaya Shukla[1], Geetanjali Arora[1], Prakash P. Kotwal[2], Rakesh Kumar[1], Arun Malhotra[1], Guru Pad Bandopadhyaya[1]

1. Department of Nuclear Medicine and
2. Department of Orthopedics, All India Institute of Medical Sciences, New Delhi: 110029, India

***

Keywords: Hydroxypropyl-β-cyclodextrin
- Nanoparticles
- ^{1}HNMR
- Infection imaging
- MBP
- Docking

Correspondence address:
Dr Guru Pad Bandopadhyaya, PhD Professor (Radiopharmacy)
Department of Nuclear Medicine, All India Institute of Medical Sciences New Delhi 110029, India
E-mail: guru47@gmail.com
Tel: 9111-26594322,
Fax: 9111-26588663

Received:
10 September 2010
Accepted:
30 September 2010

Abstract

Breast milk oligosaccharides act as soluble receptors for different pathogens which protect the newborn child from infection. The differentiation between loosening of prosthesis due to infective pathology septic or otherwise aseptic plays an important role in the patient management. We have labeled hydroxypropyl-β-cyclodextrin, oligosaccharide derivative, with technetium-99m (^{99m}Tc-HPβCD). The quality control of ^{99m}Tc-HPβCD was done by ITLC and characterized by electron microscopy and ^{1}H-nuclear magnetic resonance. The route of excretion of ^{99m}Tc-HPβCD nanoparticulate radiopharmaceutical was assessed in rats. Nanoparticles ^{99m}Tc HPβCD were injected in human subjects with clinically confirmed infected knee joints. Docking studies were done for ligand - protein interaction. The ^{99m}Tc-HPβCD was stable with good radiochemical yield (>98%) at pH 4.0 and 6.5. For single patient dose, 0.5-1.0mg HPβCD quantity was sufficient. ^{99m}Tc HPβCD was observed to form nanoparticles of 60-180μm. The ^{1}H NMR studies revealed the binding of ^{99m}Tc at C-8/H-8 position of HPβCD. The excretion of ^{99m}Tc HPβCD showed renal route of excretion. Docking studies demonstrated the interaction between HPβCD and bacterial maltose binding protein (MBP). The differentiation between septic and aseptic loosening was also evident on single photon emission tomography (SPET). *In conclusion*, these data indicated that ^{99m}Tc HPβCD is a promising radiopharmaceutical and may serve as molecular nanoprobe for infection imaging.

Hell J Nucl Med 2010; 13(3):218-223 • Published on line: 25-11-10

Introduction

The binding of streptococcus pneumonia, enteropathogenic E.coli and haemophilus to their receptors is inhibited by human breast milk oligosaccharides [1]. Human breast milk, having more than 130 oligosaccharides may act as soluble receptors for different pathogens, thus increasing the resistance of breast-fed infants [2]. The presence of oligosaccharides binding proteins on bacterial membranes has been reported [3]. In the initiation of any bacterial infection, the bacteria encounter with mucosal epithelial barrier of the human host. After bacterial adherence, the epithelial cells initiate a non-specific or innate immune response by producing pro inflammatory factors. The adherence of bacteria to human cells is mediated by bacterial membrane and it produces inflammatory responses to bacterial infections which can be utilized in detection or elimination of invading microorganism [4].

It is seen that many of obsessed patients end up with hip and/or knee prosthesis. Common complication of prosthesis is associated with loosening of prosthesis. This loosening can be with infection (septic loosening) or without any infection (aseptic loosening). Clinically, it is difficult to differentiate these two conditions. There are many non invasive modalities such as indium-111/ technetium-99m white blood cell labeling (^{111}In / ^{99m}Tc labeled WBC), fluorine-18 fluorodeoxyglucose (^{18}F-FDG) and technetium-99m methylene diphosphonate (^{99m}Tc-MDP) imaging have been used in the past with varying success in differentiating aseptic verses septic loosening [5-10]. ^{111}In or ^{99m}Tc labeled white blood cells WBC have some drawbacks, such as labeling patient's own blood, the risk of infection from exogenous microorganisms during in vitro labeling, cross-contamination with other patient's blood, and the considerable cost of the technique. As of now there is not a foolproof technique except operative culture sensitivity for detection of the underlying pathology which when negative is considered aseptic. Therefore there is a need for a test which can be useful in differentiating aseptic from septic loosening, noninvasively.

Maltose binding protein (MBP) is a monomeric periplasmic binding protein on bacterial cell membrane and plays an important role in active transport and bacterial chemotaxis. Furthermore the blocking of binding sites on bacterial surfaces can be achieved by using low molecular

weight oligosaccharides which prevent bacterial adherence. Maltose binding protein also binds to cyclic maltodextrins like cyclodextrins [3]. They do not induce any chemotactic response. The binding of cyclodextrin, dextrin and other oligosaccharide derivatives to maltose binding protein of various bacteria has been reported [11]. The binding proteins of ABC-transporter of gram positive bacteria also exhibit high similarity with maltose binding proteins (MBP) of gram negative bacteria and contains a cyclodextrin-binding site, too.

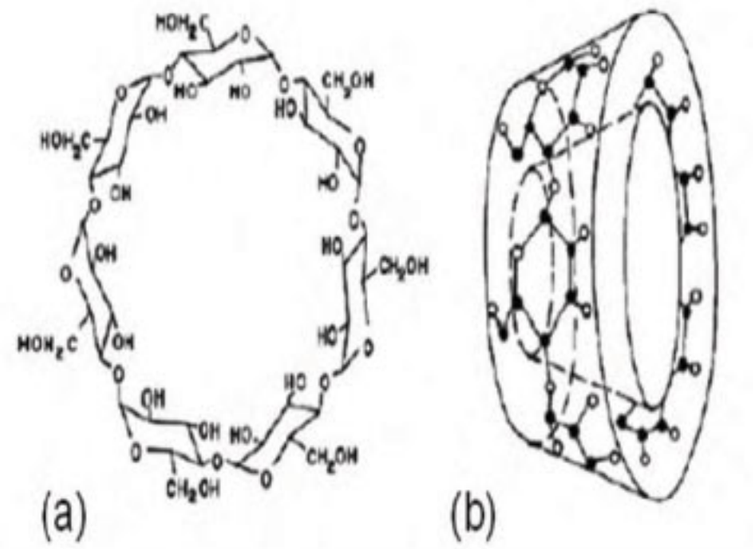

Figure 1. (a) Chemical structure of HPβCD and (b) orientation of molecules (toroid shaped).

Cyclodextrins are water-soluble cyclic oligosaccharides. The three dimensional molecular configuration of hydroxypropyl-β-cyclodextrin (HPβCD) is a toroid or cub shaped (Fig. 1) with hydrophilic exterior and relatively hydrophobic interior cavity. Cyclodextrins consist of 6, 7, or 8 (α, β and γ, respectively) D-glucopyranosyl units connected by alpha-(1, 4) glycosidic linkages [12]. The modified cyclodextrins, such as hydroxypropyl β-cyclodextrin and sulphobutyl β-cyclodextrin, are regarded as safe for parenteral use and are preferred over natural cyclodextrins because of most extensive collection of safety data with no adverse reactions reported [13-16]. The recommended parenteral human dose in 5% solution in water is 0.5 g/kg/day for 4 days. No clinically significant adverse affects were observed in these parenteral and oral studies [12, 16]. The presence of free hydroxyl groups is essential for cyclodextrin metabolism in periplasmic and cytoplasm spaces, aerobically and anaerobically. With this background we labeled HPβCD with $^{99m}TcO_4^-$ pertechnetate. After proper quality control procedures; albino wistar rats were injected with ^{99m}Tc-HPβCD to study the route of its excretion.

Materials and methods

Materials

Hydroxypropyl beta cyclodextrin was procured from Sigma-Aldrich (USA), stannous chloride from Sigma-Aldrich, ^{99}Mo-^{99m}Tc generator from Amrol (Turkey). All other chemicals used were of analytical reagent-grade. The binding of HPβCD to MBP of bacteria was demonstrated by computational method using Autodock programme in linux operating system. Crystallographic coordinates of MBP have been taken from the Brookhaven Protein Data Bank (pdb) and their reference number of Crystallographic structure is 1DMB.

Radiolabelling and in vitro stability

Hydroxypropyl beta cyclodextrin (10mg) was dissolved in 2.4mL sterile, pyrogen free water. The labeling of HPβCD was done by stannous chloride reduction method using freshly eluted $^{99m}TcO_4^-$ from MON-TEK ^{99}Mo-^{99m}Tc generator, Monrol Nuclear Products Inc (Turkey). Twenty five micrograms (μg) freshly prepared stannous chloride, in dil HCl (0.05N), was added. The solution was divided into six parts. The pH of solutions was maintained to 4, 6.5 and 8 and $^{99m}TcO_4$ (185MBq) was added in each vial and passed through a 0.22 micron filter. The radiopharmaceutical purity was evaluated by instant thin layer chromatography-silica gel (ITLC-SG) strips on a TLC scanner (Bioscan 2000, USA) using methyl ethyl ketone as a solvent front. The radiochemical stability was also assessed up to 6h. All experiments were done in triplicates.

Physical characteristics

Physical characteristics of HPβCD and ^{99m}Tc-HPβCD were examined by transmission electron microscope (TEM). The aqueous solution of HPβCD was stained with 1% (w/v) phospho-tungustic acid (negative staining), placed on a carbon film coated grid and examined under a 60kV Philips CM10 TEM to determine the size and surface morphology.

Single dose preparation

For single dose preparation, 0.05 -1.0μg quantity of HPβCD was taken for radiolabeling with ^{99m}Tc (7.4MBq). The radiochemical yield was assessed by ITLC on a TLC scanner (bioscan 2000, USA) using methyl ethyl ketone as a solvent front. The experiments were done in triplicates.

Proton nuclear magnetic resonance (^{1}H-NMR) studies

Studies of ^{1}H-NMR of HPβCD and ^{99m}Tc-HPβCD were done on lyophilized radiolabelled solution. The ^{1}H-NMR spectra were recorded on a vertical bore 400MHz (9.4T) high-resolution NMR spectrometer (Bruker, Switzerland) equipped with a broad band inverse probe. A 5mM HPβCD was prepared in 600μL of deuterated water (D_2O), and transferred to 5mm NMR tubes for NMR experiments. The one-dimensional ^{1}H-NMR spectra were recorded with a 90° pulse with solvent presaturation. Typical acquisition parameters used for 1D-NMR experiments were: pulse width, 5.8μs, number of data points, 32K, spectral width, 5000Hz and number of scans, 32-64. Receiver gain was optimized in each instance to obtain the best signal to noise ratio. A constant temperature of 25ºC was maintained by using a temperature controller.

Animal studies

Wistar rats (n=3) of 250±25g body weight were obtained from the Institute Animal House (India) and put under standard laboratory conditions (12h light/dark cycle, ambient temperature 25±2^{0}C) with free access to standard rat chow and water. Each rat was anaesthetized with intraperitoneal injection of Na-pentobarbitone (35mg/kg body weight). The tail of the rats was washed with xylon and savlon so that the tail vein was well visualised. Whole body images were made at 15min, 1h and 3h post administration of 7.4MBq ^{99m}Tc-HPβCD, in order to determine gross distribution of ^{99m}Tc-HPβCD. The planner images of rats were monitored by using a

dual head gamma camera (Mill VG, G E Electronics, Hyfa, Israel) with low energy all purpose (LEAP) collimator.

Infection imaging with ^{99m}Tc-HPβCD

The approval to use HPβCD in human subjects was taken from Drug Controller of India and the permission to use ^{99m}Tc-HPβCDin human subjects was obtained from Institutional Clinical Ethical Clearance Committee. Subjects with histological proven knee prosthesis infection were chosen for the study. The studies were conducted in dual head gamma camera using low energy high resolution collimator.

In-siloco studies/ Docking studies

Ligand-protein docking experiment was studied by using autodock 4 program on auto dock tool (ADT) in Linux operating system. Crystallographic coordinates of MBP have been taken from the Brookhaven Protein Data Bank (pdb) (USA) and the reference number was 1DMB. The HPβCD was drawn by Chemdraw program and three dimensional structures were taken as ligand. Hydrogen atoms were added and Gasteigen charges were assigned. Since MBP is a monomeric protein, the grid box was selected covering the whole protein. The docking was done for 10 genetic algorithms. Minimum energy state (most stable) ligand-protein complex was chosen. Ligand–protein contacts were derived with the help of LPC software [17].

Radiolabeling and in vitro stability

The radiopharmaceutical, ^{99m}Tc-HPβCD showed more than 99% labeling efficiency at pH 4, 6.5 and at all time points (Fig.1).

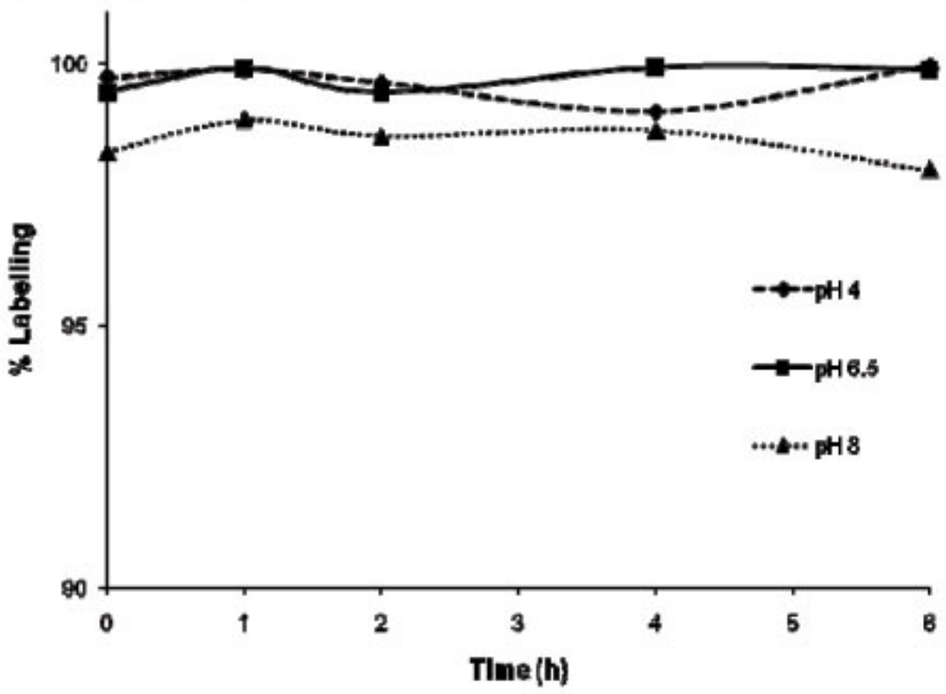

Figure 2. Labeling efficiency of HPβCD with ^{99m}Tc at pH-4.0, 6.5 and 7.0.

The labeling efficiency was more than 99% up to 4h however, it was a little less (97.97%) after 6h at pH 8 (Table 1). The radiopharmaceutical was stable at all pH during the study period.

Single dose preparation

The radiochemical yield was more than 98% with 0.5 mg HPβCD, more than 99% when 0.6mg HPβCD and around 100% when 0.8 mg HPβCD (Fig. 2). There was no change in radiochemical yield with increase in HPβCD quantity. For a single patient dose, preparation 0.6-0.8mg was sufficient.

Table 1. *Radiolabeling efficiency of ^{99m}Tc-HPβCD at pH 4.0, 6.5 and pH 8.0*

pH	15 min % (±s.d)	1 h % (±s.d)	2 h % (±s.d)	4 h % (±s.d)	6 h % (±s.d)
4.0	99.74 (±0.22)	99.88 (±0.15)	99.64 (±0.30)	99.09 (±1.53)	99.95 (±0.04)
6.5	99.47 (±0.76)	99.91 (±0.09)	99.44 (±0.27)	99.92 (±0.09)	99.89 (±0.05)
8.0	98.31 (±0.44)	98.92 (±0.12)	98.62 (±0.52)	98.72 (±0.62)	97.97 (±1.41)

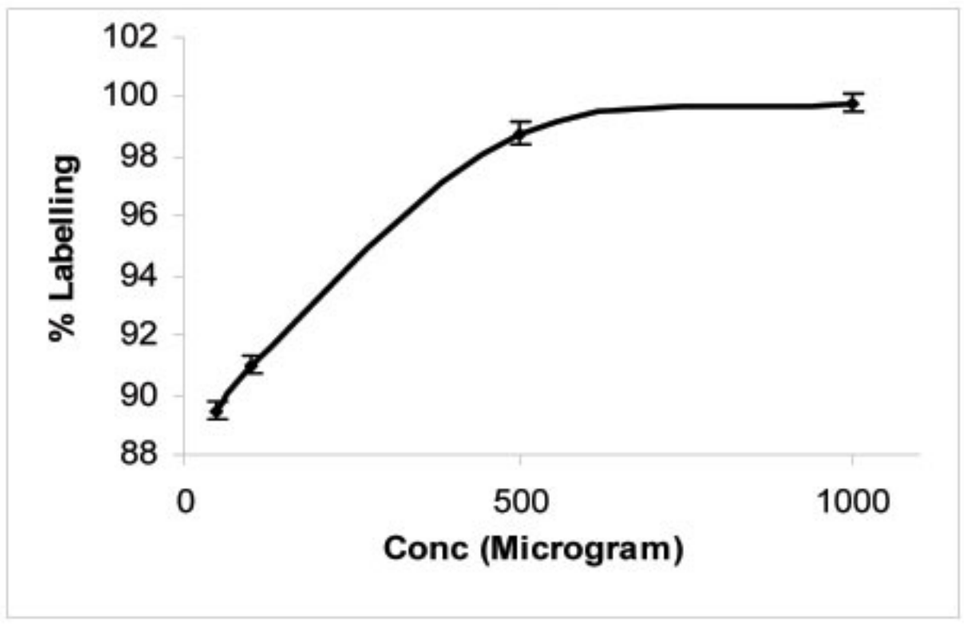

Figure 3. Amount of HPβCD required for a single dose preparation.

Characterization

The TEM micrograph of negatively stained HPβCD and ^{99m}Tc-HPβCD solutions demonstrated the nano sized particles of 60 nm-180 nm (Fig. 4). ^{1}H chemical shifts of HPβCD, before and after radiolabeling with ^{99m}Tc, were demonstrated by 1D ^{1}H NMR (Fig. 5 a and b) and depicted in Table 2.

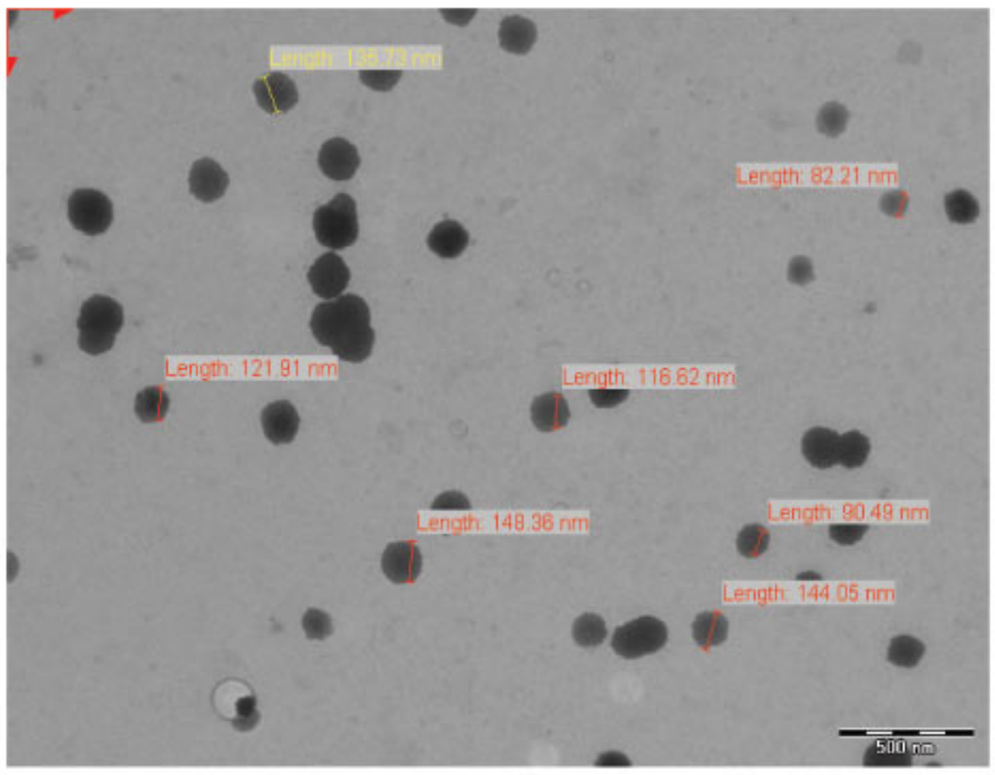

Figure 4. Transmission electron micrograph of HPβCD nanoparticles.

The protons of HPβCD were assigned using COESY connectivity. The insignificant proton shift was observed in protons H-1 to H-7 of HPβCD and ^{99m}Tc HPβCD (Table 2). HPβCD is repeated units of seven glucopyranosyl units which are arranged in a ring connected by alpha-(1,

4) glycosidic linkage. The H-8 protons of glucopyranosyl units experience upfield and downfield shift in the presence of $^{99m}TcO_4^-$ as shown in Table 2.

(a)

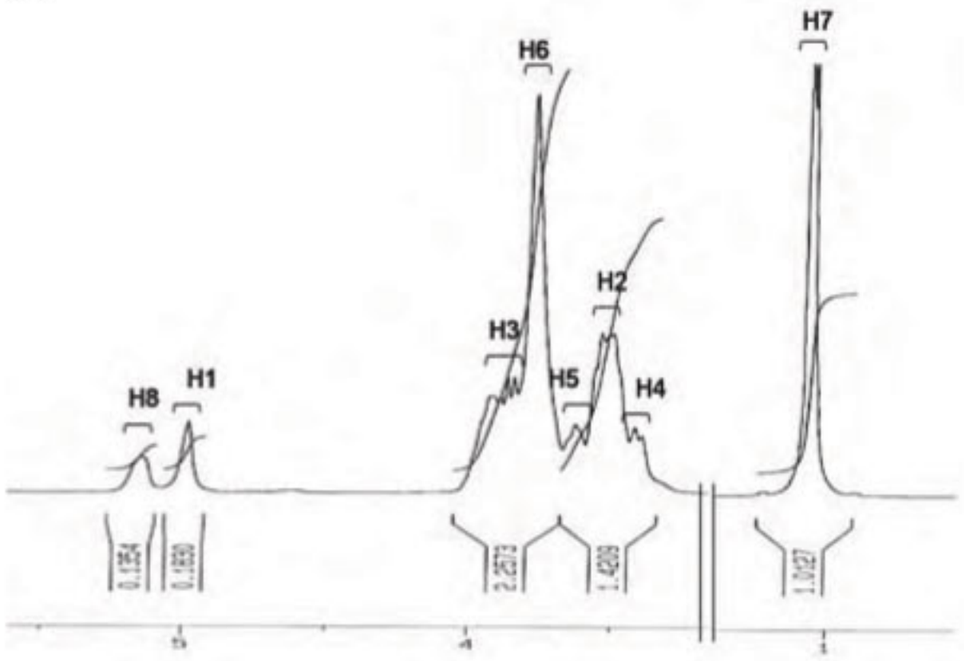

(b)

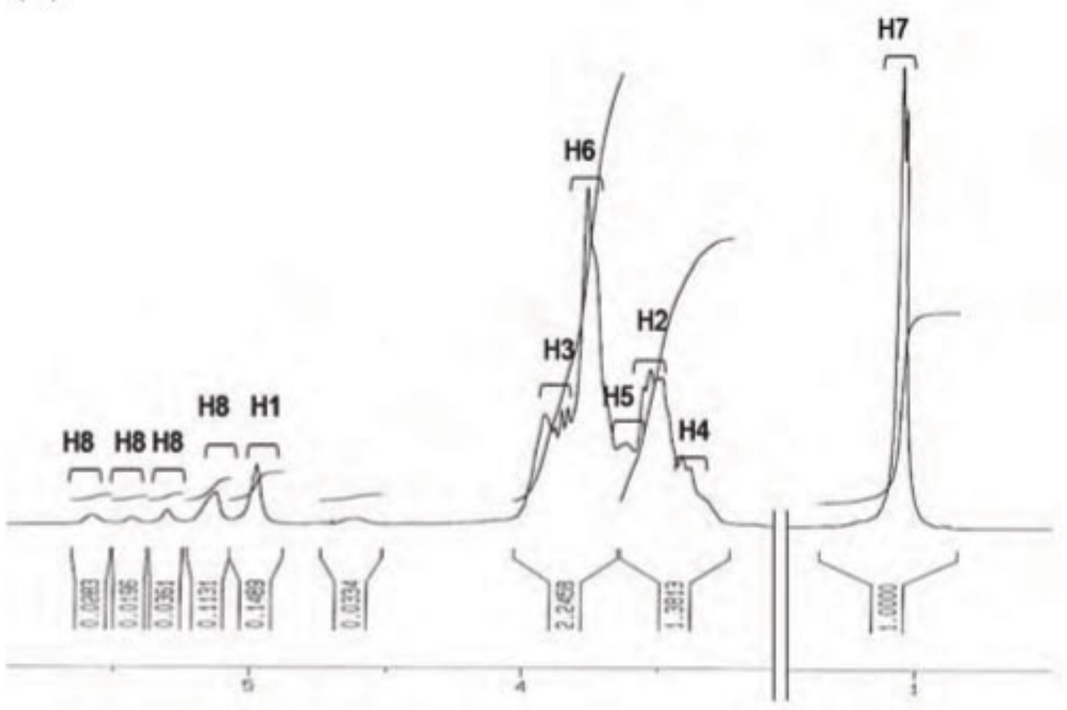

Figure 5. (a)^{1}H NMR spectra of HPβCD. (b)^{1}H NMR spectra of ^{99m}Tc-HPβCD.

Animal studies

The 15min image showed the blood pool activity with high concentration of ^{99m}Tc-HPβCD in kidneys and blad der (Fig. 6a). The 1h image showed the high renal uptake of ^{99m}Tc-HPβCD and clearance (Fig. 6b). The 3h image showed high concentration of ^{99m}Tc-HPβCD in the urinary bladder with good washout from the kidneys (Fig. 6c).

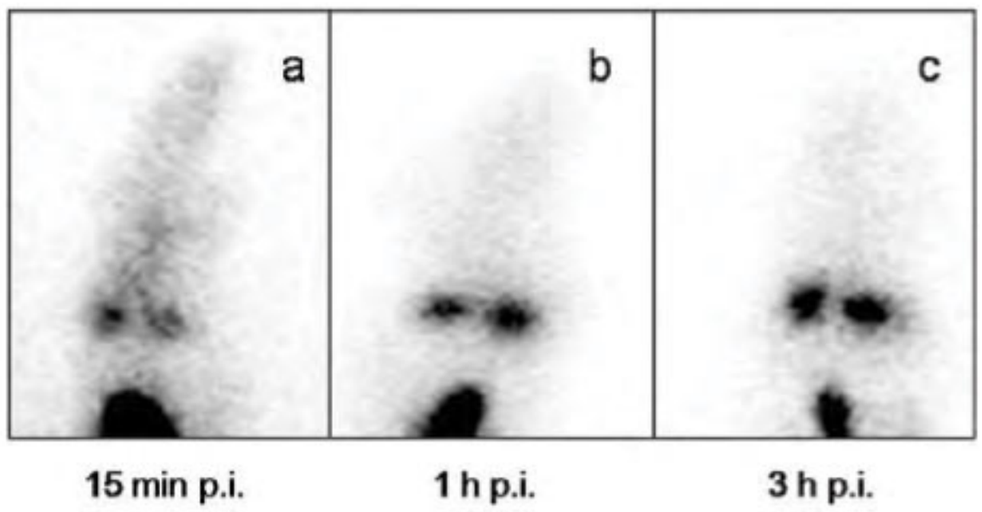

Figure 6. Gamma camera images of rats injected with 7.4MBq of ^{99m}Tc-HPβCD.

Infection imaging with ^{99m}Tc HPβCD

There was marked increased uptake of ^{99m}Tc HPβCD, in the patient with bilateral total knee joint replacement and histologically proven infection, in the left knee. However, there was no uptake in right knee (Fig. 7).

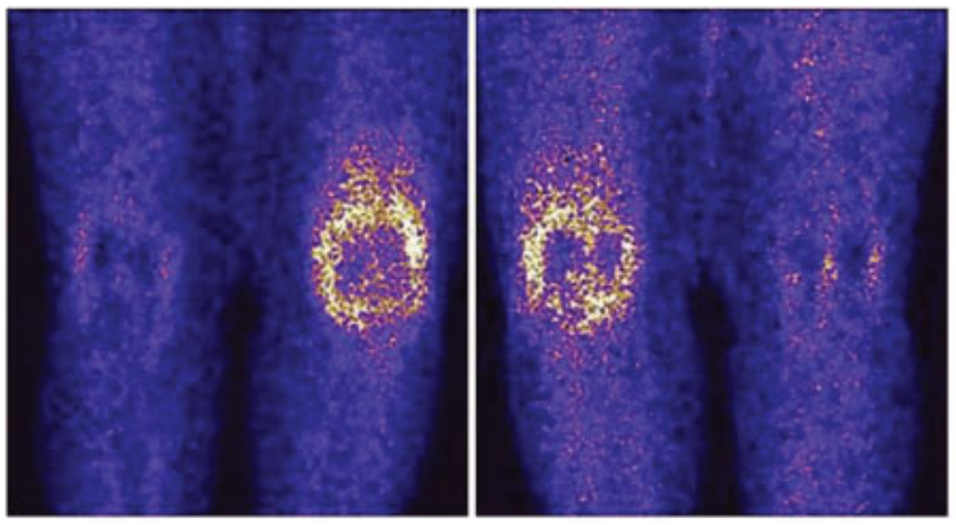

Figure 7. ^{99m}Tc-HPβCD images in human subjects (a) with prosthesis infection, (b) with no prosthesis infection.

Docking analysis

The structures after docking were analyzed on the basis of energy levels. The lowest energy co-ordinates were taken for ligand protein interaction on LPC server which demonstrated hydrophobic, hydrophilic and van der Waals interactions between ligand and amino acid residues of MBP (Fig. 8, Table 3). HPβCD was located at the base of the cleft, similar to betacyclodextrin position, on MBP.

Results

The radiopharmaceutical (^{99m}Tc-HPβCD) showed more than 99% labeling efficiency at pH 4, 6.5 and at all time points (Fig. 2). The labeling efficiency was more than 99% up to 4h. However, it was little declined (97.97%) after 6h at pH 8 (Table 1). The radiopharmaceutical was stable between pH 4.0-8.0 during our studies. The radiochemical yield was more than 98% with 0.5mg HPβCD, more than 99% with 0.6mg HPβCD and around 100% with 0.8mg HPβCD (Fig. 3). There was no change in radiochemical yield with increase in HPβCD quantity. The ^{99m}Tc-HPβCD was stable up to 6h. For single patient dose preparation 0.6-0.8mg was sufficient (Fig. 3). TEM micrograph of negatively stained HPβCD and ^{99m}Tc-

Table 2. *^{1}HNMR proton shift (Δδ) of HPβCD in the presence of ^{99m}Tc*

Proton	HPβCD ppm	^{99m}Tc HPβCD ppm	Δδ ppm
H-1	4.970	4.974	0.004
H-2	3.499	3.499	0.000
H-3	3.853	3.872	-0.019
H-4	3.411	3.410	0.001
H-5	3.588	3.538	-0.050
H-6	3.764	3.730	-0.034
H-7	1.029	1.025	-0.004
H-8	5.154	5.128	-0.026
		5.307	+0.153
		5.436	+0.282
		5.564	+0.410

HPβCD solutions demonstrated the nano sized particles of 60-180nm (Fig. 4).

Table 3. *Interaction of ligand with protein residues*

Residue		Dist	Surf	Specific contacts		
				HB	Phob	DC
211A	PRO*	2.5	31.8	+	-	-
212A	GLY*	2.8	28.7	+	-	-
220A	ALA*	3.9	19.4	-	-	+
221A	PHE*	2.6	65.2	+	-	+
222A	ARG*	2.6	110.6	+	+	-
223A	GLU*	2.6	106.8	+	-	+
226A	ASN*	4.1	11.4	-	-	+
227A	TYR*	2.9	50.4	+	-	-
228A	SER*	2.5	44.9	+	-	-
229A	LEU*	4.4	3.8	+	-	-
230A	PRO*	3.3	20.1	-	-	+

The 1H chemical shifts of HPβCD, before and after radiolabeling with ^{99m}Tc, were demonstrated by 1D ^{1}H NMR (Fig. 5 a, b) and depicted in Table 2. The protons of HPβCD were assigned using COESY connectivity. The insignificant proton shift was observed in protons H-1 to H-7 of HPβCD and ^{99m}Tc-HPβCD (Table 2). The structure of HPβCD is repeated units of seven glucopyranosyl units which are arranged in a ring connected by alpha-(1, 4) glycosidic linkage (Fig. 1). The H-8 protons of glucopyranosyl units experience up field and downfield shift in the presence of $^{99m}TcO_4^-$ as shown in Table 2. The 1H-NMR spectra demonstrated overlapping signals of repeated glucopyranosyl units. No significant shift was observed at H-1 to H-7 protons of HPβCD and ^{99m}Tc-HPβCD, but prominent shift was observed at H-8 proton of ^{99m}Tc-HPβCD. The H-8 protons of glucopyranosyl units experienced shift in the presence of $^{99\ m}TcO_4^-$ (Fig. 5, Table 2).

The 15min image showed the blood pool activity with high concentration of ^{99m}Tc-HPβCD in kidneys and urine bladder (Fig. 6a). The 1h image showed the high renal uptake of ^{99m}Tc-HPβCD and clearance from the kidneys in the rat model (Fig. 6b). However, 3h image showed high concentration of ^{99m}Tc HPβCD in urinary bladder with maximum clearance from the kidneys (Fig. 6c). The activity in thyroid was not visualized throughout the study and indicated proper labeling and in vivo stability of ^{99m}Tc-HPβCD.

There was marked increased uptake of ^{99m}Tc-HPβCD in the patient's left knee having clinically proven infection (Fig. 7). However, there is no uptake in the right knee due to the absence of microbial infection. Maltose binding protein has two globular domains. The orientation of ^{99m}Tc- HPβCD on MBP was earlier determined by NMR studies (19-20). The βCD was at the base of the cleft either with direct βCD-protein hydrogen bond or water-mediated hydrogen bonds (21). In our studies minimum energy coordinates of HPβCD-MBP complex were taken to study interactions of MBP and HPβCD by using LPC server (17). The established interactions were hydrogen bonds, van der Waals interactions and hydrophilic interactions (Fig. 8, Table 3).

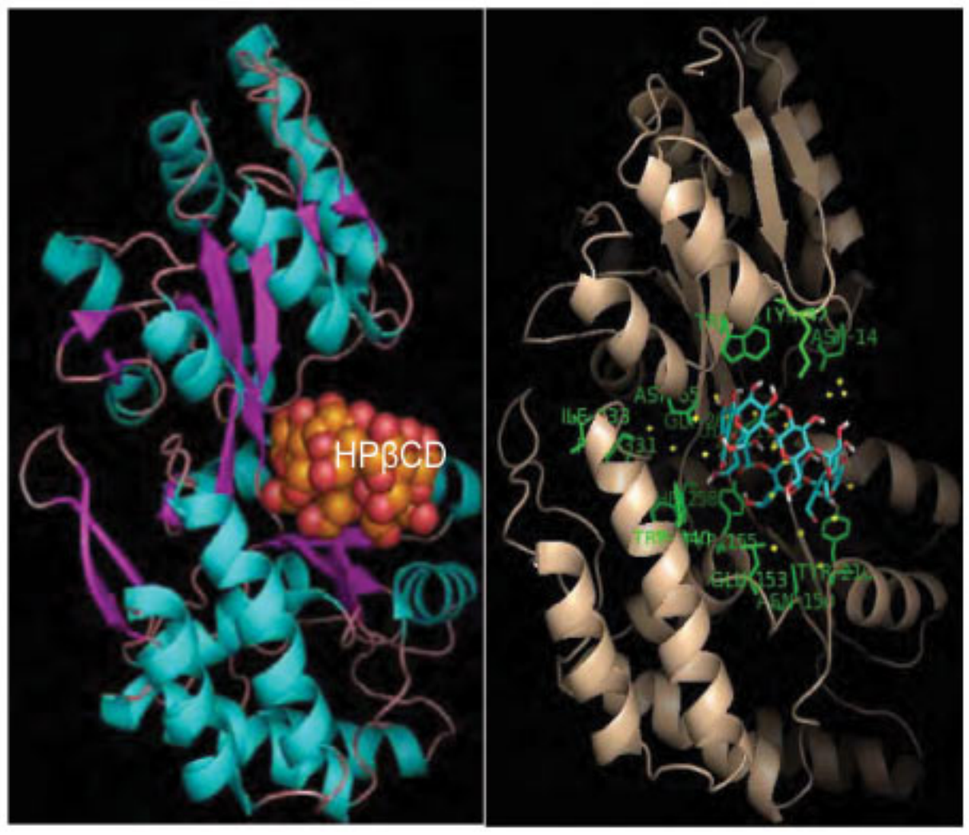

Figure 8. (a) The localization of HPβCD (spheres) at MBP (cartoon) cavity and (b) interaction of amino acid side chains of MBP with HPβCD (sticks) derived from docking experiment.

Discussion

The nano structures of 60-180nm under the electron microscope demonstrated the formation of aggregated particles of HPβCD and ^{99m}Tc-HPβCD. González-Gaitano et al (2002) have studied the aggregation processes of natural and modified cyclodextrins (CDs) in diluted aqueous solutions by photon correlation spectroscopy. They demonstrated that α-, β -, and γ-CD form large polydispersed, aggregated nanoparticles of 200-300 nm. But the partially substituted CDs (Methyl- β -CD and HPβCD) form weaker aggregates. Smaller aggregates of 60-180nm were formed by using substituted cyclodextrin, HPβCD [18].

The ^{1}HNMR spectra demonstrate overlapping signals of repeated glucopyranosyl units. There was no significant shift was observed at H-1 to H-7 protons of HPβCD and ^{99m}Tc HPβCD. A prominent shift was observed at H-8 proton of ^{99m}Tc-HPβCD. The H-8 protons of glucopyranosyl units experienced shift in presence of $^{99m}TcO_4^-$ (Table 2). On the basis long stability period of ^{99m}Tc-HPβCD and shift at H-8 position, it could be concluded that strong H-bonding existed between glucopyranosyl unit and ^{99m}Tc. The ITLC and TEM of ^{99m}Tc-HPβCD demonstrated high stablily and formation of nanoaggregates of 60-180 nm.

^{99m}Tc-HPβCD showed good renal activity and clearance from the kidneys. No thyroid activity was visualized at any time point which indicated good in vivo stability. The uptake of ^{99m}Tc-HPβCD was facilitated by the nanoparticles due to increased permeability of inflamed area but the retention of ^{99m}Tc-HPβCD in the knee joint with prosthesis infection was possibly due to the ligand protein intetraction between ^{99m}Tc-HPβCD and MBP or similar receptor proteins having maltodextrin binding sites on membranes of infection causing microbes [19]. However there was no

radiopharmaceutical uptake at non infected knee which confirmed the interaction of ^{99m}Tc-HPβCD with bacterial/microbial MBP. Maltose binding protein has two globular domains. The orientation of cyclodextrin on MBP was earlier determined by NMR studies [19-21]. Shraff et al (1995) demonstrated that βCD bind with K_d of the same order to MBP. The βCD was at the base of the cleft either with direct βCD-protein hydrogen bond or water-mediated hydrogen bonds. In our studies minimum energy coordinates of HPβCD-MBP complex were taken to study interactions of MBP and HPβCD by using LPC server. The established interactions were hydrogen bonds, van der Waals interactions and hydrophilic interactions (Table 2). As HPβCD-MBP interactions are similar to βCD-MBP as shown by our docking experiment, we can also assume that some amino acid side chains (MBP) and HPβCD interactions are mediated by water molecules. The interactions between HPβCD and MBP stabilize HPβCD in the cleft of MBP.

Cyclodextrin (^{99m}Tc-HPβCD) can easily be labeled with diagnostic isotope (^{99m}Tc) may become a potential molecular probe for infection imaging and also be utilized further to differentiate infected lesions from cancerous lesions that can not be detected by other modalities like MRI or PET/CT imaging.

In conclusion, ^{99m}Tc-HPβCD is cost effective as compared to other radiopharmaceuticals like ^{99m}Tc-HMPAO, ^{18}F-FDG etc, can easily be labeled with $^{99m}TcO_4^-$ and has a renal route of clearance. The localization of ^{99m}Tc hydroxypropyl-β-cyclodextrin is possibly due to its binding to the maltose binding proteins present on infection causing microbial membrane. ^{99m}Tc-HPβCD is a promising radiopharmaceutical and may serve as molecular nanoprobe for infection imaging.

Acknowledgement

We are thankful to the Indian Council for Medical Research for funding the study. We are also thankful to the Department of Nuclear Magnetic Resonance, Electron Microscope Facility and Animal House Facility of our institute, All India Institute of Medical Sciences. Our special thanks to Prof Debasisa Mohanty, National Institute of Immunology for docking experiment

Bibliography

1. McVeagh P, Miller, JB. Human milk polysaccharides: only the breast. *J Paediatr Child H* 1997; 33: 281-6.
2. Newburg DS. Do the binding properties of oligosaccharides in milk protect human infants from gastrointestinal bacteria? *J. Nutr* 1997; 127: 980S-4S.Pajatsch M, Gerhart M, Peist R et al. The periplasmic cyclodextrin binding protein cyme from *klebsiella oxytoca* and its role in maltodextrin and cyclodextrin transport. *J. Bacteriol* 1998; 180: 2630-5.
4. Kinz C, Rudloff S. Biological functions of oligosaccharides in human milk. *Acta Paediatr* 1993; 82: 903-12.
5. Weiss PE, Mall JC, Hoffer PB et al. Technetium-99m methylene diphosphonate bone imaging in the evaluation of total hip prosthesis. *Radiology* 1979; 133: 727-9.
6. Utz JA, Calvin EG, Lull RJ. Natural history of technetium- 99m MDP bone scan in asymptomatic total hip prostheses. *J Nucl Med* 1982; 23: 28-9.
7. Williamson BR, McLauchlin RE, Wang GW et al. Radionuclide bone imaging as a means of differentiating loosening and infection in patients with a painful hip prosthesis. *Radiology* 1979; 133: 723-5.
8. Mulamba L, Ferrant A, Leners N et al. Indium-111 leukocyte scanning in the evaluation of painful hip arthroplasty. *Acta Orthop Scand* 1983; 54: 695-7.
9. Magnuson JE, Brown ML, Hauser MF et al. ^{111}In-labeled leukocyte scintigraphy in suspected orthopedic prosthesis infection: Comparison with other imaging modalities. *Radiology* 1988; 168: 235-9.
10. Dumarey N, Egrise D, Blocklet D et al. Imaging Infection with ^{18}F-FDG–labeled leukocyte PET/CT: Initial experience in 21 Patients. *J Nucl Med* 2006; 47: 625-32.
11. Kamionka A, Dahl MK. Bacillus subtilis contains a cyclodextrin-binding protein which is part of a putative ABC-transporter. FEMS Microbiol Lett 2001; 204: 55-60.
12. Rajewski RA, Stella VJ. Pharmaceutical application of cyclodextrins.2. In vivo drug delivery. *J Pharm Sci* 1996; 85: 1142-68.
13. Irie T, Uekama K. Pharmaceutical applications of cyclodextrins. 3. Toxicological issues and safety evaluation. *J Pharm Sci* 1997; 86: 147-62.
14. Stella VJ, Lee HK, Thompson DO. The effect of SBE4-β-CD on i.v. Methylprednisolone pharmacokinetics in rats: Comparison to a co-solvent solution and two water-soluble prodrugs. *Int J Pharm* 1995; 120: 189-95.
15. Brewster ME, Hora MS, Simpkins JW, Bodor N. Use of 2-hydroxypropyl-beta-cyclodextrin as a solubilizing and stabilizing excipient for protein drugs. *Pharm Res* 1991; 8: 792-5.
16. Pitha J, Gerloczy A, Olivi A. Parenteral hydroxypropyl cyclodextrins-intravenous and intracerebral administration of lipophiles. *J Pharm Sci* 1994; 83: 833-7.
17. Sobolev V, Sorokine A, Prilusky J et al. Automated analysis of interatomic contacts in proteins. *Bioinformatics* 1999; 15: 327-32.
18. González-Gaitano G, Rodríguez P, Isasi JR et al. The aggregation of cyclodextrins as studied by photon correlation spectroscopy. J Incl Phenom Macro Chem 2002; 44: 101-5.
19.Hall A, Thorgeirsson TE, Lu J et al. The presence of oligosaccharides binding proteins in bacterial membranes have been reported. *J Biol Chem* 1997; 272: 17610-4.
20. Sharff AJ, Rodseth LE, Szmelcman S et al. Refined Structures of Two Insertion/Deletion Mutants Probe Function of the Maltodextrin Binding Protein. *J Mol Biol* 1995; 246: 8-13.
21. Skrynnikov NR, Goto NK, Yang D et al. Orienting Domains in Proteins Using Dipolar Couplings Measured by Liquid-state NMR: Differences in Solution and Crystal Forms of Maltodextrin Binding Protein Loaded with β-Cyclodextrin. *J Mol Biol* 2000; 295: 1265-73.